

# An Introduction to MEBT for J-PARC and Its Upgrade Design

WANG Sheng<sup>1;1)</sup> FU Shi-Nian<sup>1</sup> Taiko Kato<sup>2</sup>

<sup>1</sup> (Institute of High Energy Physics, CAS, Beijing 100049, China)

<sup>2</sup> (KEK, High Energy Accelerator Research Organization, 1-1 Oho, Tsukuba-shi, Ibaraki-ken 305-0801, Japan)

**Abstract** The medium-energy beam-transport line (MEBT) plays an important role in reducing the beam loss in the Japan Proton Accelerator Research Complex (J-PARC). A MEBT was designed and constructed, with good beam matching and lower beam loss. A brief introduction to the MEBT and its beam test results are given. To further reduce the beam loss during the transient time of the chopper, a medium-energy beam-transport line with an anti-chopper has been designed. It accomplishes three tasks: matching the beam from the RFQ to the acceptance of the DTL, chopping the beam to produce gaps for injection into the rapid cycling ring which follows the linac, and returning the partially deflected beam back to the acceptance of the DTL. An RF chopper and an anti-chopper have been adopted in the beam line, and the optimization of the design of the chopper cavity is discussed. Details of the beam dynamics analysis are given.

**Key words** MEBT, chopper, beam loss control

## 1 Introduction

The Japan Proton Accelerator Research Complex (J-PARC) consists of a 400MeV linac, a 3GeV rapid cycling ring, and a 50GeV main ring. A 400MeV linac is used as the injector of a 3GeV rapid cycling ring. The linac comprises a  $H^-$  ion source with a pulse length of 500 $\mu$ s at 50Hz repetition rate, a 324MHz RFQ with an output energy of 3MeV, a 50MeV DTL and a 200MeV SDDL at the frequency of 324MHz, and an annular coupled structure with an output energy of 397MeV at 972MHz. The linac provides a beam of 50mA in peak current and 0.7mA in average current.

From the point of view of either the pulse current or the average current, the beam intensity in the linac of the J-PARC project is high. Beam loss control is a very essential requirement in accelerator design and performance to avoid strong radioactivity induced by lost particles. In the linac design of the J-PARC project, the Medium-Energy Beam-Transport line (MEBT), between RFQ and DTL, plays an impor-

tant role in the beam loss control. It accomplishes beam matching and chopping. These two tasks have a close relation with beam-loss control. Beam matching is very important to minimize the growth of emittance and avoid beam-halo formation, which has been recognized as one of the major causes for beam loss<sup>[1]</sup>. Clean chopping is also a key point for beam loss control. In the J-PARC project, 500 $\mu$ s long macropulses from the ion source need to be chopped into sub-pulses for injecting into the following 3GeV rapid-cycling ring. The sub-pulse consists of a 455ns long pulse and a 358ns gap, as indicated in Fig. 1. The chopped pulse should have a clean cut at the head and the tail of the pulse so as to avoid beam loss at

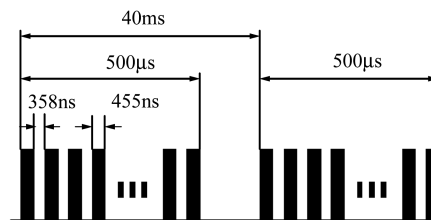


Fig. 1. The required time structure of the macro and micro beam pulses.

Received 16 May 2005

1) E-mail: wangsheng@ihep.ac.cn

later parts of the linac or during the injection into the ring.

A MEBT for J-PARC was designed<sup>[2]</sup> and constructed, with good beam matching and lower beam loss. An RF deflector is adopted as a chopper<sup>[3]</sup> for getting a clean cut at the head and tail of the pulse. The beam line with an RF chopper has been successfully commissioned<sup>[4]</sup> with 20mA H<sup>-</sup> beam current. Fig. 2 shows the structure of the chopped beam at the exit of MEBT. However, there are still some unstable particles, which are partially deflected during the rise and fall time of the chopping field (three bunches during the rise time and three bunches during fall time), they may be accelerated to high energy and lost or get into the ring. When the beam current is increased to the designed goal of 50mA, these unstable particles may bring much more trouble.

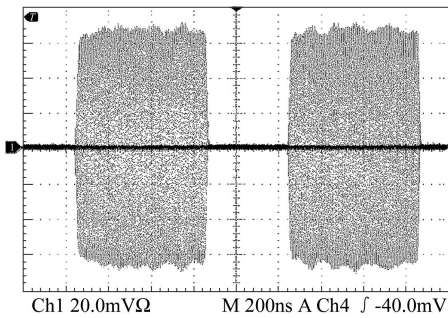


Fig. 2. The structure of a chopped beam measured by BPM at the exit of MEBT (200ns/div).

To further reduce the number of these unstable particles in MEBT, the adoption of an anti-chopper is a good choice for decreasing the number of the unstable particles. Theoretically, using an anti-chopper can cancel all of the unstable particles produced during the transient time.

Based on the previous design of MEBT, a MEBT with an anti-chopper was designed. It accomplishes matching and chopping, and eliminate all of the transient part of the chopped beam. To maintain the beam quality, the length of the transport line is not increased too much, in spite of adding an anti-chopper. This benefits from the asymmetric design. The details of the design are described in this paper, and the optimization of the design of the chopper cavity is discussed. Details of the beam dynamics

analysis are given.

## 2 Design of the beam line

### 2.1 The adoption of the asymmetric scheme

For returning partly deflected beams back to the beam axis by using an anti-chopper, the symmetric design is a direct idea of using an anti-chopper, just like in the case of the SNS MEBT<sup>[5]</sup>. When using a symmetric design, the arrangement of elements between the chopper and anti-chopper is symmetric. However, some extra elements are needed just to maintain the symmetry. The key problem is that the symmetric arrangement makes the envelope at the location of the anti-chopper hard to control, and the aperture of the anti-chopper is a bottle neck of MEBT. The adoption of the asymmetric scheme is a good choice.

### 2.2 Feasibility of the asymmetric scheme

For adoption of the asymmetric design, two points should be investigated first: if it can surely return any partly deflected beam back to the beam axis, and finding the relation between the chopper and the anti-chopper.

Consider a beam line with two choppers and two anti-choppers. Let  $x$  be the deflection direction;  $(x_1, x'_1)$ ,  $(x_2, x'_2)$ ,  $(x_{a1}, x'_{a1})$  and  $(x_{a2}, x'_{a2})$  are the beam centroid at the two choppers and the two anti-choppers respectively, where  $x_1 = 0$  and  $x'_1 = 0$ . Let

$$R = \begin{bmatrix} r11 & r12 \\ r21 & r22 \end{bmatrix},$$

be the transfer matrix from the second chopper to the first anti-chopper; then,

$$\begin{bmatrix} x_{a1} \\ x'_{a1} \end{bmatrix} = \begin{bmatrix} r11 & r12 \\ r21 & r22 \end{bmatrix} \begin{bmatrix} x_2 \\ x'_2 \end{bmatrix}. \quad (1)$$

Assume that  $x'_0$  and  $kx'_0$  are the deflected angle provided by the chopper and the anti-chopper respectively,  $L$  is the distance between the two choppers and  $L_a$  is the distance between two the anti-choppers. One can obtain  $x_2 = x'_0 L$  and  $x'_2 = 2x'_0$ . To deflect the beam back to the axis, it is required that  $x_{a1} = kx'_0 L_a$

and  $x'_{a1} = 2kx'_0$ . Combine with Eq. (1), we have

$$\begin{bmatrix} kx'_0 L_a \\ 2kx'_0 \end{bmatrix} = \begin{bmatrix} r11 & r12 \\ r21 & r22 \end{bmatrix} \begin{bmatrix} x'_0 L \\ 2x'_0 \end{bmatrix},$$

or

$$\begin{bmatrix} kL_a \\ 2k \end{bmatrix} = \begin{bmatrix} r11 & r12 \\ r21 & r22 \end{bmatrix} \begin{bmatrix} L \\ 2 \end{bmatrix}. \quad (2)$$

Because Eq. (2) does not depend on  $x'_0$ , we illustrate that, for any given  $L$ ,  $L_a$  and  $k$ , any deflected beam can be deflected back to the axis. Since matrix  $R$  that satisfies Eq. (2) is not unique, there is a space to optimize the design when the asymmetric scheme is adopted.

### 2.3 Design of MEBT with an anti-chopper

A modified TRACE3D<sup>[2]</sup> is used to describe the deflection behavior of the chopper and the anti-chopper. It includes the element of an RF deflector. The field distribution of the deflector was obtained from MAFIA results, including the fringe fields beside the deflecting electrode. The beam parameters at

the entrance of the MEBT (exit of RFQ) are listed in Table 1.

Table 1. The beam parameters at the MEBT entrance.

$I/\text{mA}$	$\varepsilon_{\text{RMS}}^{x,y}/(\pi\text{mm}\cdot\text{mrad})$	$\varepsilon_{\text{RMS}}^z/(\pi\text{MeV}\cdot^\circ)$
50	0.200	0.150

A design of MEBT with an anti-chopper is shown in Fig. 3. The first half of the beam line, upstream of element 18, mainly aims at obtaining a large separation between the chopped beam and the unchopped beam at element 18. A scraper is located next to the element 18. In this part, the arrangement of elements remains the same as that of the previous MEBT design, and uses the same RF deflectors as a chopper. Regardless the head and the tail of a bunch, the edge separation between a full-chopped beam and a normal beam is 4mm at the scraper, when both RF deflectors have a deflecting field of 1.9MV/m (corresponding to 27kW driving power). For deflecting the head and the tail of the bunch, much more driving power is needed.

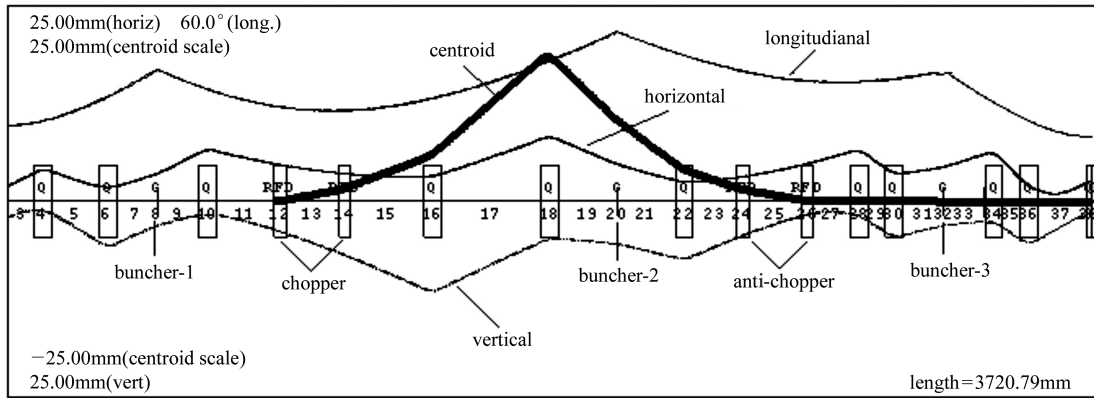


Fig. 3. TRACE 3-D output of MEBT with an anti-chopper.

The beam profiles in the  $z$ ,  $x$  and  $y$  directions are shown respectively. The coarse line traces the beam centroid deflected by two RF choppers and two RF anti-choppers.

The second part of the beam line, downstream element 18, accomplishes two tasks: returning a partly deflected beam back to the beam axis and matching the unchopped beam with the acceptance of DTL.

A similar type of RF deflector as the chopper is adopted as an anti-chopper. Taking advantage of the asymmetric scheme, the deflecting field can be different from that of the chopper. In the design of Fig. 3, a deflecting field of 1.7MV/m is adopted in the anti-chopper. When the driven power of the chopper

is changed, tuning the beam line parameter of element 18th to 25th can satisfy the requirement of anti-chopper, without changing the driving power of the anti-chopper. Thus, the driving power of the anti-chopper can be fixed. The other four quadrupoles, downstream the anti-chopper, are used to match the transverse phase space to the acceptance of DTL.

There are three bunchers in the beam line to keep the bunch length from increasing too much. Two bunchers are needed for matching the longitudinal

phase space to the acceptance of DTL. Three bunchers make it easy to control the bunch length at the deflector, and also make it possible to make the bunch length close to each other at the chopper deflectors and the anti-chopper deflectors.

## 2.4 Elements used in the beam line

Table 2 gives the total number of elements used in the beam line with the anti-chopper, compared with the previous no anti-chopper beam line. Except for the deflector, all of the elements are the same as those used in the no anti-chopper beam line.

In the previous design, to decrease the number of the partly deflected bunches, the deflector reaches a very fast rise time. Because of adopting an anti-chopper, it is possible to allow proper longer rise time by changing the coupling of deflector cavity, to obtain higher deflection field.

Table 2. Elements number used in the beam line.

anti-chopper	$Q$	deflector	buncher	length/m
yes	10	4	3	3.6
no	8	2	2	2.9

## 3 The optimization of anti-chopper

A similar type RF deflector is adopted as an anti-chopper. The gap between two electrodes of the anti-chopper deflector is increased to 12mm, while that of chopper deflector is 10mm. The larger gap is required to ensure no particle is lost on the electrode. To get the same deflecting voltage, the larger gap means larger driving power requirement. The maximum capability of the up-to-date solid power supply is 30kW. To decrease the demand of the input power, some further optimizations are proposed based on the previous design<sup>[3]</sup>.

To minimize the demand power  $P$ , a large value of  $Z/Q_0$  should be pursued according to an approximate relation

$$P \cong \frac{V^2}{\omega_0 \tau (Z/Q_0)}$$

in which  $V$  is the deflecting voltage,  $\omega_0$  the frequency,  $\tau$  the rise time,  $Z$  the transverse shunt impedance and  $Q_0$  the unloaded  $Q$  value of the deflector cavity. To get the higher value of  $Z/Q_0$ , the cuboid electrode is

replaced by a stem plus electrode structure, as showed in Fig. 4. The size of the top surface of the electrode is kept unchanged.

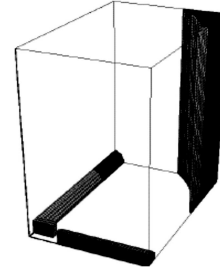


Fig. 4. The structure of an RF deflector with the newly designed electrode.

Table 3 shows the comparison of the  $Z/Q_0$  between cuboid electrode structure and stem structure. The value of  $Z/Q_0$  is increased by a factor of 17%.

Table 3. The  $Z/Q_0$  with different electrode structures.

type	$Q_0$	$Z$	$Z/Q_0$
cuboid	$1.102 \times 10^4$	$4.87 \times 10^6$	442
stem	$1.034 \times 10^4$	$5.35 \times 10^6$	517

## 4 Beam dynamics simulation

The beam dynamics of the beam line was studied using PARMILA. Fig. 5 shows the simulation results of the emittance growth along MEBT. Although an anti-chopper is added and the total length is increased to 3.5m, the RMS emittance growth is still less than 16%. No extra emittance growth exists compared with that of the previous no anti-chopper design.

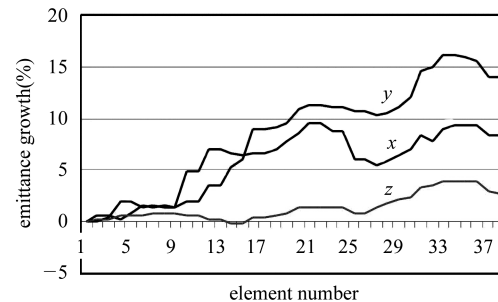


Fig. 5. RMS emittance growth along the beam line.

Fig. 6 shows the phase space of a 60% deflected beam at the entrance of DTL. The partly deflected beam is returned back to the beam axis by the anti-chopper, within the acceptance of DTL.

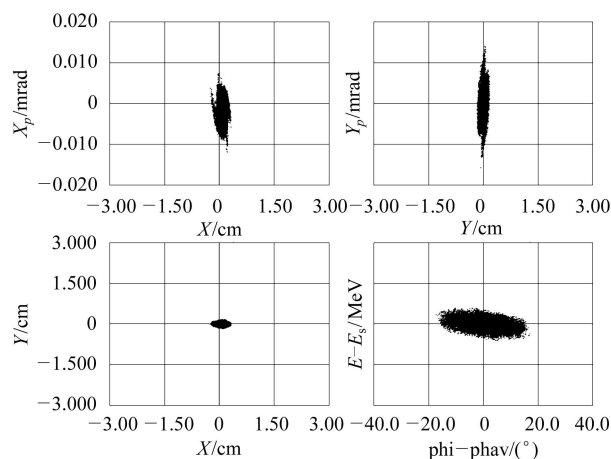


Fig. 6. Phase space of a beam deflected by the chopper and the anti-chopper at entrance of the DTL.

## 5 Conclusion

A brief introduction to MEBT and its beam test results are given. To further reduce the beam loss during the transient time of the chopper, based on the previous MEBT design, a MEBT with an anti-chopper has been designed for matching and clean chopping beam. Taking advantage of the asymmetric scheme, the design is much more flexible and can use different deflectors for the chopper and the anti-chopper. To decrease the demanded power of anti-chopper deflector, some further optimisations for RF deflector are proposed. Simulation results show that there is no extra emittance growth due to the use of an anti-chopper, and that all of partly chopped beam can be returned back to the acceptance of DTL.

## References

- 1 Yamazaki Y. Design Issues for High-Intensity, High Energy Proton Accelerators. Proc. of 1996 Inter. Linac Conf. Geneva, 1996, 26
- 2 Fu S, Kato T. Nucl. Instrum. Methods, 2001, **A457**: 423—437
- 3 Fu S, Kato T. Nucl. Instrum. Methods, 2000, **A440**: 296—306
- 4 WANG S et al. Beam Commissioning of the J-PARC Linac Medium Energy Beam Transport at KEK-II. Proceeding of the 28th Japan Linac Meeting. WP-53, July, 2003, Tokai, Japan
- 5 Staples J, Oshatz D et al. Design of the SNS MEBT. LINAC'2000. Monterey, MOD18, August, 2000

# 日本质子加速器研究设施中的中能束流传输线及其升级设计

王生<sup>1;1)</sup> 傅世年<sup>1</sup> 加藤隆夫<sup>2</sup>

1 (中国科学院高能物理研究所 北京 100049)

2 (日本高能加速器研究机构 筑波 305-0801 日本)

**摘要** 中能束流传输线(MEBT)在日本质子加速器研究设施(J-PARC)中对控制束流损失起到非常关键的作用. 中能传输线已经成功设计和建造, 并进行了束流实验. 简要介绍了中能传输线及其束流实验的结果. 为进一步减少和消除传输线中的束流切割器的上升和下降过程中产生的不稳定粒子, 以满足更高流强下的束损要求, 给出了一个带有反束流切割器的中能传输线的升级设计, 该设计已被用作该项目的备用方案. 升级设计的中能传输线要完成三个任务: 完成从RFQ到DTL的束流相空间匹配; 利用束流切割器把束流切割成注入快循环时所需要的束流结构, 以及利用反束流切割器把束流切割器上升和下降时间段产生的部分偏转的不稳定粒子作用回DTL的相空间接收度内, 以减少和避免粒子丢失. 在该中能传输线中, RF偏转器被用来作为束流切割器和反束流切割器. RF偏转器是中能传输线中最关键的部件, 进一步讨论了RF偏转器作为反束流切割器的优化设计. 也给出了该传输线的动力学分析的结果.

**关键词** 中能束流传输线 束流切割器 束损控制

2005 - 05 - 16 收稿

1) E-mail: wangs@ihep.ac.cn